# Permeable TAD boundaries and their impact on genome-associated functions

Li-hsin Chang, Daan Noordermeer

Received: 5 June 2024 | Revised: 12 July 2024 | Accepted: 17 July 2024

DOI: 10.1002/bies.202400137

BioEssays

HYPOTHESES

Insights & Perspectives

# Permeable TAD boundaries and their impact on genome-associated functions

**Li-Hsin Chang**[1,2] | **Daan Noordermeer**[3]

[1]MRC Molecular Haematology Unit, MRC Weatherall Institute of Molecular Medicine, Radcliffe Department of Medicine, University of Oxford, Oxford, UK

[2]Blood and Transplant Research Unit in Precision Cellular Therapeutics, National Institute of Health Research, Oxford, UK

[3]CEA, CNRS, Institute for Integrative Biology of the Cell (I2BC), Université Paris-Saclay, Gif-sur-Yvette, France

**Correspondence**
Li-Hsin Chang, MRC Molecular Haematology Unit, MRC Weatherall Institute of Molecular Medicine, Radcliffe Department of Medicine, University of Oxford, OX3 9DS Oxford, UK.
Email: li-hsin.chang@ndcls.ox.ac.uk

Daan Noordermeer, CEA, CNRS, Institute for Integrative Biology of the Cell (I2BC), Université Paris-Saclay, 91198 Gif-sur-Yvette, France.
Email: daan.noordermeer@i2bc.paris-saclay.fr

**Funding information**
Agence Nationale de la Recherche, Grant/Award Numbers: ANR-21-CE12-0034, ANR-21-CE12-0034, ANR-22-CE12-0016, ANR-22-CE14-0021; Blood and Transplant Research Unit in Precision Cellular Therapeutics

## Abstract

TAD boundaries are genomic elements that separate biological processes in neighboring domains by blocking DNA loops that are formed through Cohesin-mediated loop extrusion. Most TAD boundaries consist of arrays of binding sites for the CTCF protein, whose interaction with the Cohesin complex blocks loop extrusion. TAD boundaries are not fully impermeable though and allow a limited amount of inter-TAD loop formation. Based on the reanalysis of Nano-C data, a multicontact Chromosome Conformation Capture assay, we propose a model whereby clustered CTCF binding sites promote the successive stalling of Cohesin and subsequent dissociation from the chromatin. A fraction of Cohesin nonetheless achieves boundary read-through. Due to a constant rate of Cohesin dissociation elsewhere in the genome, the maximum length of inter-TAD loops is restricted though. We speculate that the DNA-encoded organization of stalling sites regulates TAD boundary permeability and discuss implications for enhancer–promoter loop formation and other genomic processes.

**KEYWORDS**
3D genome organization, Cohesin, CTCF, enhancer–promoter looping, gene regulation, loop extrusion, Topologically Associating Domains

## 1 | INTRODUCTION

Mammalian genomes are hierarchically organized within the cell nucleus; ranging from the smallest order of organization (i.e., chromatin) to sub-Megabase (Mb) Topologically Associating Domains (TADs), A/B compartments and chromosome territories. Moreover, promoters and enhancers can form DNA loops to transfer regulatory information. In many cases, enhancers are located at large genomic distances from their target genes (in some cases over a Megabase) and can bypass more proximally located genes to interact with their targets.[1–4]

An important participant in the process of enhancer–promoter looping (EP-looping) in mammalian cells is the CTCF (CCCTC-binding factor) insulator protein. The binding of CTCF to its complex and non-symmetric binding site in-between enhancers and promoters was initially reported to block EP-loop formation.[5–7] Since then, regions surrounded by convergently oriented CTCF binding sites were shown to appear as "pyramids" or "triangles" in Hi-C interaction matrices.[8–13]

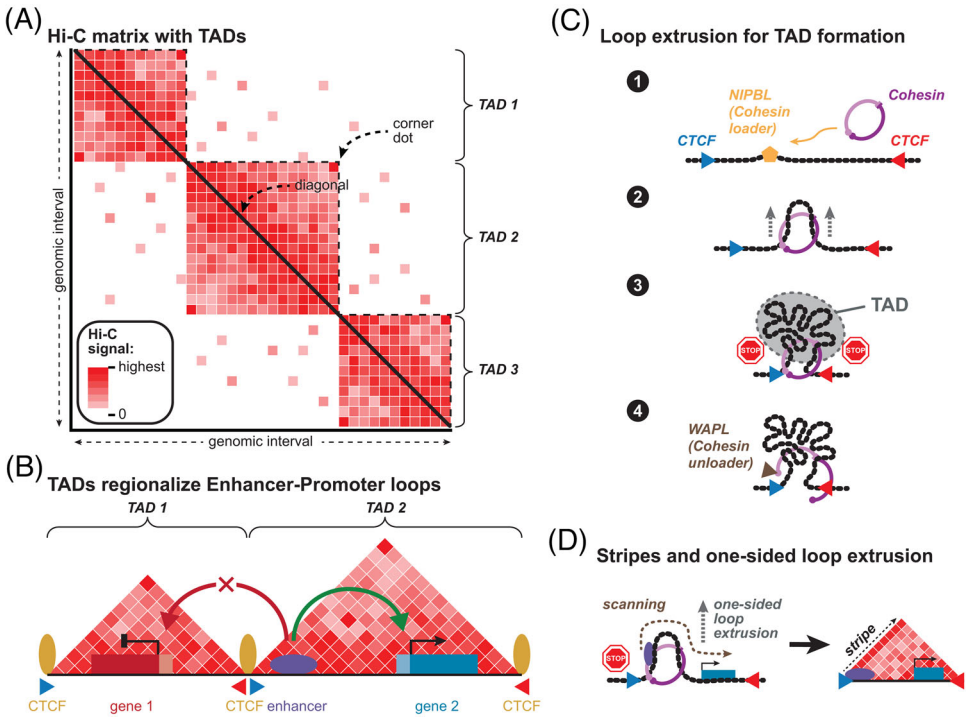


**FIGURE 1** TADs appear as insulated domains that are formed by a process of Cohesin-mediated loop extrusion. (A) Schematic Hi-C interaction map, showing the presence of three insulated Topologically Associating Domains (TADs) that appear as pyramids with enriched intradomain interactions along the diagonal. Arrows highlight the diagonal (black line) and the presence of a corner dot at the summit of TADs. The Hi-C interaction matrix is a mirror-image across the diagonal; only the top-right part along the diagonal, after 45° tilting, will be shown in follow-up figures. (B) Enhancer–promoter loops can be formed within TADs but are discouraged between TADs through the binding of the CTCF insulator proteins at TAD boundaries. Arrowheads below CTCF binding sites indicate the expected orientation of the sites. (C) Schematic overview of TAD formation by loop extrusion and its blocking at sites that bind the CTCF insulator protein. In a first step, the ring-shaped Cohesin protein complex is loaded onto the chromatin by the NIPBL loading factor. Next, a bidirectional DNA loop is extruded until correctly oriented CTCF binding sites—on one or both sides—are encountered, resulting in blocking of the extrusion process. The process ends when the Cohesin complex is unloaded by the WAPL release factor. Importantly, release (step 4) can occur before the Cohesin complex is blocked on one or both sides (e.g., during step 2 or 3). (D) Preferential loading of the Cohesin complex next to a CTCF binding site promotes one-sided loop extrusion. Such sites are visible as "stripes" in the Hi-C map and allow an enhancer to scan the chromatin for its target genes until a CTCF binding site on the other side is encountered.

Such regions, generally in the order of 500 kb to 1 Mb in size, represent TADs (also known as "loop-domains") where intradomain interactions are increased over interactions with the surroundings (Figure 1A). Within TADs, enhancers and their promoters are grouped together, thereby regionalizing the EP-loop landscape.[3,14,15] The CTCF binding sites that form the separation between neighboring TADs are known as TAD boundaries or TAD borders[8,16] (Figure 1B).

Despite the prominent visibility of TADs in Hi-C maps, the chromatin within these domains is only moderately insulated from the surroundings (around twofold increased intradomain contacts), raising the question of how such limited insulation can prevent the formation of EP-loops between neighboring TADs.[16] Multiple studies have confirmed that the disruption of TAD boundaries, consistently involving CTCF binding sites, can modify gene activity in disease settings, including ectopic gene activation through enhancer hijacking.[17–22] In this manuscript, with a focus on mammalian cells, we discuss recent evidence that most TAD boundaries are built-up from arrays of CTCF binding sites that modulate a permeable separation between neighboring domains. Using examples from the literature, we speculate how this combinatorial binding constitutes a DNA-encoded means for the regulation of EP-loop dynamics and other genome-associated processes.

## 2 | TADS AND LONG-RANGE EP-LOOPS ARE DYNAMIC STRUCTURES THAT ARE FORMED BY LOOP EXTRUSION

TADs are formed by a dynamic and continuously ongoing process of loop extrusion (Figure 1C).[23–30] This process starts with the loading of the ring-shaped Cohesin protein complex onto the chromatin by the NIPBL loading factor. Cohesin is preferentially loaded at enhancers and promoters where paused RNA polymerase II accumulates, yet loading appears to occur elsewhere in the genome as well.[31–37] Next, the Cohesin complex starts the extrusion of chromatin, thereby creating a DNA loop that can increase in size in both directions. Within TADs, this extrusion process is required for bringing distant enhancer and promoter pairs in contact (approximately >100-kb distance).[38,39]

When Cohesin encounters a correctly oriented CTCF protein on one side, loop extrusion is blocked in that direction. This blocking at a TAD boundary prevents the formation of loops between enhancers and promoters in neighboring domains. Yet, when blocked on one side, loop extrusion can continue in the other direction (one-directional extrusion) until the complex encounters a correctly oriented CTCF protein on the other side as well.[23,24,27–30] When Cohesin is blocked on both sides, the CTCF-bound anchors will be in spatial proximity, which creates a noticeable "corner dot" at the summit of the TAD in the Hi-C map (Figure 1A–C). When Cohesin is preferentially loaded next to a CTCF-bound site, it will immediately start the extrusion of a one-directional loop, which appears as a "stripe" or "FIRE" in the Hi-C map (Figure 1D).[31,32,40] Such a mechanism allows for the one-directional "scanning" of the genome, which can be exploited by "super-enhancers" and promoters to search for their target genes within TADs.[31,41]

Importantly, at any time after loading, the Cohesin complex can be unloaded from the chromatin by its release factor WAPL.[42–45] Upon release, the loop that has been extruded will resolve. Recent live-cell imaging studies have revealed that blocking of Cohesin on both sides of a TAD is a rare event ("fully extruded loop"), making up only around 6%–25% of the time.[46,47] Combined with the low density of intra-TAD loops, in the order of 1–2 loops at any time within a single TAD on one allele in a single cell, this has resulted in the notion that TADs are statistical entities rather than insulated domains.[46–49] This has further been supported by imaging, single-cell Hi-C and multicontact 3C studies that detected a considerable variation in both TAD structure and the positioning of TAD boundaries between cells in the same population.[16,50–56] The strong depletion of loops that cross boundaries nonetheless makes TADs appear as triangles in Hi-C map, which represent an averaged description of extruded DNA loops from thousands to millions of cells. The regionalizing function of TADs is, thus, the combined outcome of Cohesin-mediated loop extrusion, to promote intra-TAD EP-loop formation, and its blocking by CTCF at TAD boundaries, to discourage inter-TAD EP-loop formation (Figure 1B,C). Besides regionalizing gene regulation, TADs and loop extrusion are involved in other genomic functions as well, including DNA repair, replication, and recombination (see Refs. [57–59] and below).

## 3 | CTCF BINDING CREATES PERMEABLE TAD BOUNDARIES

Whereas the importance of CTCF-mediated blocking of loop extrusion at certain TAD boundaries is well established, the inner workings of this process remain less understood. The analysis of CTCF binding reveals a noticeable enrichment of clustered CTCF binding sites within several tens of kilobases around TAD boundaries.[16,56,60–63] Indeed, around 90% of TAD boundaries are spread out over extended genomic intervals of up to 150 kb, where multiple CTCF binding sites are grouped together. The remaining 10% of boundaries appear as "sharp," with generally a single CTCF binding site located in between neighboring domains (manuscript submitted). Although the disruption of CTCF binding can perturb the insulation between neighboring TADs, more detailed dissections of TAD boundaries revealed that the removal of individual CTCF binding sites causes only a minor increase in inter-TAD contacts. Instead, a complete fusion of neighboring TADs requires the removal of all CTCF binding sites at these complex boundaries.[18,22,64–68] Similarly, the ectopic integration of CTCF binding sites within an existing TAD does not completely revert the formation of an existing EP-loop.[69,70] These genetics studies, thus, suggest redundancy among clustered CTCF binding sites at TAD boundaries, possibly due to an additive contribution to the separation between domains.

These observations raise the question of why the clustering of CTCF binding sites, and their potential additive contribution to TAD separation, is a feature of strong boundaries. One explanation may be related to the residence time of CTCF to its binding sites, and the resulting variation in occupation rate. Single-molecule imaging studies have determined the genome-wide DNA binding kinetics, reporting that CTCF binds in vivo to the DNA (on average) for 1–2 min at a time.[71,72] In contrast, the Cohesin complex remains associated for 15–20 min to the DNA. Cohesin may, therefore, engage in multiple cycles of loop extrusion, stalling at CTCF binding sites and restart of the extrusion process when CTCF dissociates from its binding site. Combined with the finding that CTCF binding sites are bound by the CTCF protein about 50% of the time[73] and the further influence of binding orientation.[74,75] this suggests that blocking of loop extrusion is a dynamic process that incorporates a frequent read-through of CTCF binding sites. This simplified model does not take into account that Cohesin and CTCF binding can reciprocally stabilize their association to the DNA (see, e.g.,[48,76–80] for in vivo and[74,81,82] for in vitro evidence). Support for our hypothesis may nonetheless be found in a biophysical model for loop extrusion blocking, where live-cell imaging data could only be reproduced if a single CTCF binding site had a blocking efficiency of 25%.[46] In the remainder of this manuscript, we will refer to the function of CTCF in the blocking of the extruding Cohesin complex as "stalling," to highlight the temporal nature of this process.

Previously, we reported that most TAD boundaries do not appear as sharp boundaries in the Hi-C contact map, but instead show enriched local signal around the boundary (Figure 2A).[16] This indicates that the chromatin at the boundaries is locally intermingled, thereby creating a more gradual and extended separation between the neighboring TADs over a genomic interval of 50–100 kb. Generally, multiple binding sites for CTCF can be observed within these regions (Figure 2A). To distinguish these regions from the rare "sharp" TAD boundaries, we coined the term "zones of transition."[16] To determine how individual CTCF binding sites contribute to TAD separation in these zones of transition, we developed Nano-C—a multicontact Chromosome Conformation Capture approach—to determine domain structure with single-allele and single-cell precision (Figure 2B,C).[56] The resulting multicontact hubs represent cliques of DNA fragments that were in close spatial proximity within the same cell. The analysis of large numbers of hubs in multicontact assays thereby provides information about the cell-to-cell variation of higher-order genome organization, either covering the entire genome (e.g., Refs. [83–86]) or restricted to one or few preselected genomic regions ("viewpoints"; see Refs. [53, 56, 87]).

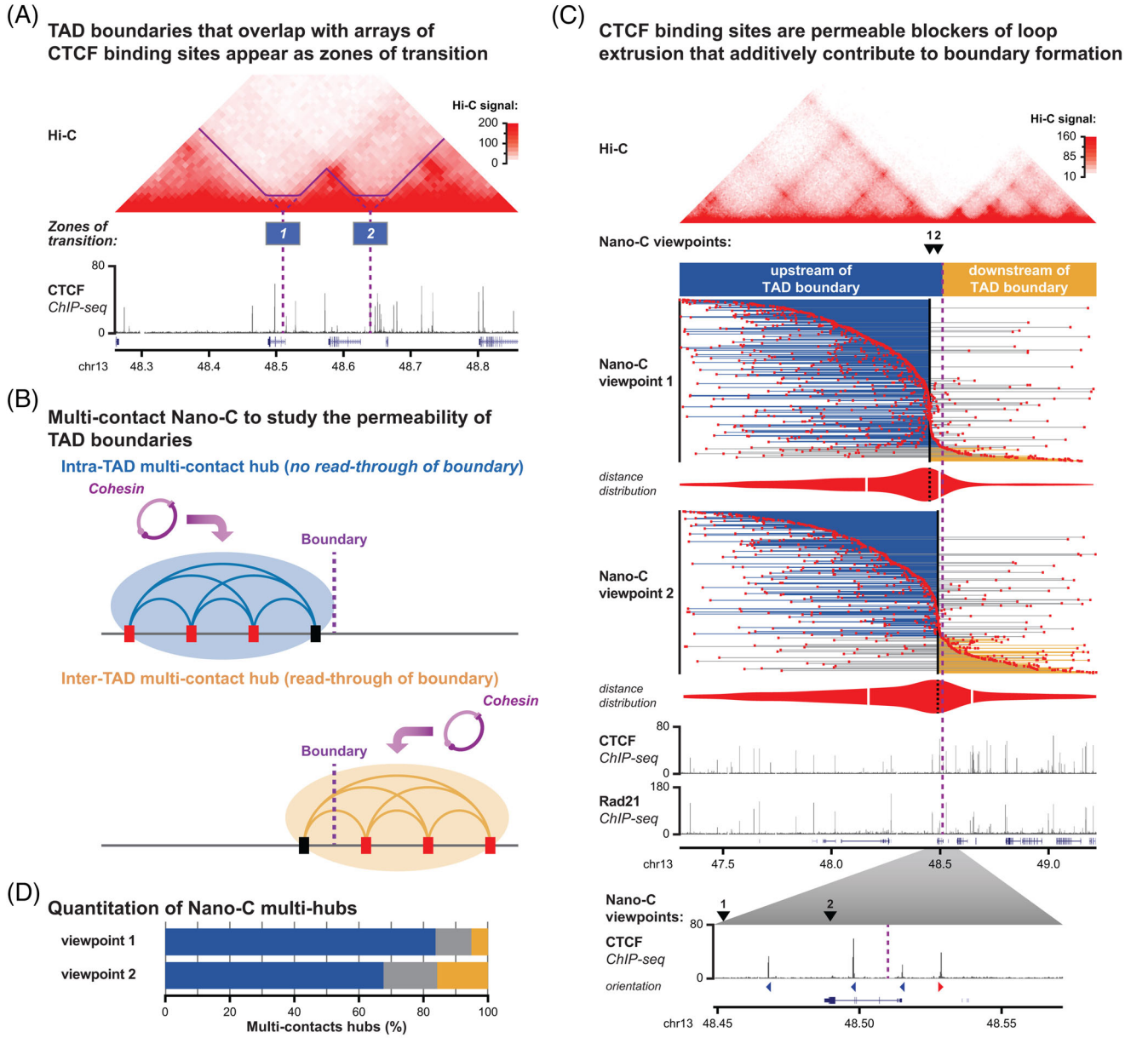


**FIGURE 2** CTCF binding sites are permeable and additively contribute to TAD separation. (A) Chromatin at TAD boundaries is locally intermingled, thereby creating "zones of transition" between neighboring TADs. Rather than a discrete separation between TADs, an elevated local signal can be observed in the Hi-C map around the two boundaries (diagonal dashed purple lines vs solid line in the Hi-C map). The TAD boundaries are indicated with the vertical purple line and the approximate extent of the zones of transition is indicated with blue boxes. CTCF binding (ChIP-seq) is indicated below, which shows the overlap between the zones of transition and arrays of CTCF binding sites. Data adapted from Chang et al.[56] (B) Outline of the multicontact Nano-C approach to determine the permeability of a TAD boundary. Nano-C identifies multicontact hubs that represent DNA fragments that simultaneously interact within a single cell. These hubs can be used to determine domain formation with single-allele and single-cell precision. For a defined site in the genome (viewpoint; black box), all interacting fragments (red boxes) are plotted on a horizontal line that represents the genomic span of the multicontact hub. In the blue example, an intra-TAD multicontact hub is formed, confirming the absence of boundary read-through. In this case, loop extrusion was initiated within the TAD on the left (approximate loading site indicated above). In the yellow example, an inter-TAD multicontact is formed, whereby the preselected viewpoint near the boundary forms a hub with fragments on the other side of the boundary. In this case, loop extrusion originated in the TAD on the right (approximate loading site above) followed by read-through of the boundary. The fraction of blue versus yellow multicontact reads is a measure of boundary permeability. **(C)** Nano-C multicontact hubs for two viewpoints that are located close to a TAD boundary, but with different numbers of CTCF binding sites that form the separation with the neighboring TAD. The TAD boundary of interest, as identified from Hi-C data (top), is highlighted with the purple dashed line. On the bottom, a zoom-in of CTCF binding (ChIP-seq) is provided, showing the presence of four CTCF binding sites around the boundary. Nano-C viewpoint 1 is located upstream of all four binding sites, whereas viewpoint 2 has three CTCF binding sites that separate it from the neighboring TAD. In the Nano-C panels, several hundreds of individual multicontacts hubs (consisting of the viewpoint and two or more interacting fragments; each hub originating from an individual cell) are stacked on top of each other. The position of the viewpoint is represented by the black vertical line. Red boxes indicate individual contacts. Multicontact hubs are sorted based on the shortest distance from the viewpoint.

We applied Nano-C to address the permeability of TAD boundaries, by determining if multicontact hubs from individual cells are strictly intra-TAD or can bridge between neighboring TADs as well (Figure 2B). The fraction of inter-TAD hubs, that is, those with contacts in neighboring TADs, subsequently provides a measure for the permeability of the boundary. We focussed our analysis on four TAD boundaries where multiple CTCF binding sites are grouped together.[56] To obtain a comprehensive view of boundary strength and the contribution of CTCF binding sites in this process, we designed multiple viewpoints at these boundaries, either in-between or just outside the arrays of CTCF binding sites. By analyzing hundreds of multicontact hubs for these viewpoints, both the permeability of the TAD boundary and the capacity of individual CTCF binding sites to contribute to loop extrusion blocking can be assessed.

As an example, we will discuss the results for two viewpoints at a TAD boundary that consists of four nearby CTCF binding sites (Figure 2C; bottom). For a viewpoint that is located upstream of the boundary, the large majority of multicontacts are intra-TAD (Figure 2C,D; blue multicontact hubs for viewpoint 1). This enrichment confirms that TADs are indeed of an insulated nature in a large fraction of cells. Nonetheless, about 5% of hubs contain the viewpoint in one TAD and all their contacts in the neighboring TAD (Figure 2C,D; yellow multicontact hubs for viewpoint 1). These inter-TAD multicontact hubs represent cells where loop extrusion read-through of the boundary has occurred (Figure 2B). Despite making up a small fraction of the total reads, the number of these hubs where the viewpoint and contacts are located in different TADs is strongly enriched.[56] These results provide a direct measurement of the permeability of the TAD boundary, thereby confirming recent live-cell imaging of boundary behavior.[46,47]

Next, we focussed on a viewpoint that is located in-between CTCF binding sites 1 and 2 and thus separated from the neighboring TAD by only three sites (Figure 2C, viewpoint 2). Here, the large majority of multicontact hubs remained intra-TAD, yet the fraction of hubs that contained all contacts in the neighboring TAD had increased to about 15% (Figure 2C,D; blue and yellow multicontact hubs for viewpoint 2). When the separation from the neighboring TAD consists of only three CTCF binding sites (instead of four), loop extrusion read-through had increased by around threefold. Individual CTCF binding sites within a zone of transition, thereby additively contribute to the overall stalling of loop extrusion and separation between the neighboring TADs.[16,56] A similar additive behavior was observed at the other three TAD boundaries that we analyzed, albeit with differences in the quantitative contribution of the individual CTCF binding sites at each boundary. Based on these outcomes, we envision a mechanism whereby the arrays of CTCF binding sites exert their function through a successive stalling of the extruding Cohesin complex. When occupied and correctly oriented, individual CTCF binding sites will have the capacity to pause the complex.[10–13,71] After a certain time though, this stalling will not be maintained and the Cohesin complex will restart its extruding activity. This loss of stalling may either be caused by the dissociation of the CTCF protein from the DNA, whose residence time at the genome-wide scale is shorter than the association of Cohesin with the DNA, or by a dissociation between the N-terminus of the CTCF protein and the Rad21 protein within the Cohesin complex.[48,71,72,74] Each stalling event prolongs the occupancy time of the Cohesin complex on the chromatin, thereby allowing its release by the dedicated WAPL release factor.[42,43] Potentially further aided by other (weaker) stalling factors like (paused) RNA polymerase II,[35,36] this creates a stop-and-go effect where each stalling event will effectively reduce the number of loops that can read-through the boundary. Nonetheless, this process of successive stalling is not completely efficient, with a small fraction of extruding Cohesin complexes achieving read-through and formation of inter-TAD loops.[56]

## 4 | DOES STALLING OF LOOP EXTRUSION REDUCE THE NUMBER OR LENGTH OF LOOPS THAT READ THROUGH BOUNDARIES?

Based on our Nano-C studies, we hypothesize that successive stalling of loop extrusion can have two nonexclusive effects on loops that achieve boundary read-through:

1. The cumulative stalling of the loop-extruding Cohesin complex at the boundary leads to an increased release from the chromatin. As a result, the number of boundary-spanning loops is reduced.
2. Stalling of the Cohesin complex at boundaries over prolonged periods of time will count towards the total residence time on the chromatin. As a result, the average length of extruded loops that cross the boundary is reduced.

Support for both effects may be found upon the depletion of the WAPL release factor, where population-averaged Hi-C experiments revealed a strong increase in the fraction of long-range DNA contacts.[44,45,87,88] Moreover, differential regulatory interactions

Blue horizontal lines indicate hubs where the viewpoint and all contacts obey the boundary (see panel (B); blue model). Yellow horizontal lines indicate hubs where the viewpoint is on the opposite side of the boundary as all its contacts (see panel (B); yellow model). Gray lines indicate mixed hubs, which are strongly depleted. Although the majority of multicontact hubs obey the boundary (blue lines), the enriched fraction of multicontact hubs that resulted from boundary read-through (yellow lines) confirm that CTCF binding sites and TAD boundaries are permeable. Comparison of viewpoint 2 to viewpoint 1 shows the fraction of yellow read has tripled, confirming the additive contribution of the intervening CTCF binding site to the separation between the TADs. This is further supported by the distance distribution, indicated below each viewpoint, which shows that intra-TAD multicontact distribution is similar for both viewpoints, whereas inter-TAD contact lengths are strongly increased for viewpoint 2. Panel reproduced, in modified form, from Chang et al.[56] (D) Quantitation of Nano-C multicontact hubs for the two viewpoints in panel (C). Color-coding of multicontact hub categories as described in the previous panel as well. Original data from Chang et al.[56]

between CTCF, the Cohesin complex and WAPL may result in the modulation of both loop number and length as well ([74–76,78] and below).

To obtain insights into the diversity of loops that are formed after a read-through of the boundary, we revisited our Nano-C results.[56,89] In normal cells, multicontact hubs within the two depicted TADs can span hundreds of kilobases (Figure 2C; a span of the individual horizontal lines that link viewpoints to their contacts). In contrast, when we performed similar experiments in cells where a functional Cohesin complex is absent (Rad21-AID degron cells[25,88]), the large majority of these long-range multicontact hubs were lost (see Ref. [56]). Consequently, the large majority of these long-range multicontact hubs are the outcome of the active loop extrusion process. To answer the question if stalling of loop extrusion at a TAD boundary reduces the length of extruded loops in the neighboring TAD, we visualized the longest distance between the viewpoints and their interacting fragments for individual Nano-C multicontact hubs (Figure 3A). Although we cannot exclude that some of these loops may represent the cumulative distance bridged between two or more loops, we previously determined that a large fraction of multicontacts represent individually extruded loops.[56] Visualization of the longest span in normal cells and in cells where a functional Cohesin complex is absent, confirms the importance of loop extrusion for bridging long distances. Indeed, in Rad21-AID cells, a curved distribution of longest distances can be observed, whereby short-range interactions are enriched both upstream and downstream from the viewpoint (Figure 3A). Interestingly though, such a decay in long-range interactions is not observed in normal cells. Instead, a more gradual reduction in loop sizes is observed for both viewpoints, with a particularly prominent change in the slope for viewpoint 1 at the TAD boundary caused by the strong reduction in loops that achieve the read-through of the boundary (Figure 3A). To determine the influence of the TAD boundary on loop length, combined with corrections for differences in the number of loops up- and downstream of the boundary and for the size of the neighboring TADs, we used a normalized signal in the range of 0–700 kb from the boundary (Figure 3B). Here, we find that the size distributions of loops that are formed after crossing the boundary are similar to those that formed within the same TAD. Moreover, we find no difference between the two viewpoints (Figure 3B). This analysis, therefore, supports a model whereby stalling at TAD boundaries reduces the number of loops that read-through the boundary, but does not influence the size of the loops that are subsequently formed. Unexpectedly, the linear shape of these curves suggests that dissociation of the actively extruding Cohesin complex is not a random process, but rather that a fixed number of molecules are removed over genomic intervals of a specific length.

Based on these observations, we propose a model for the dynamics of loop extrusion and Cohesin removal, whereby TAD boundaries primarily function to reduce the number of loops that cross the boundary (Figure 3C). In contrast, boundaries do not noticeably affect the length of the loops that are formed after read-through. In this model, large numbers of (stalled) Cohesin molecules are removed at the zones of transition surrounding TAD boundaries. Yet, a smaller and constant number of extruding Cohesin molecules is removed elsewhere in the genome as well. As a result, the number of Cohesin molecules that achieve boundary read-through will directly determine the number of inter-TAD loops at a given distance from the boundary. Next, due to the constant rate of Cohesin removal after a read-through of the boundary, the number of remaining loops will indirectly determine the maximum size of extruded loops as well. Modulation of Cohesin stalling at TAD boundaries, for instance by changing the number or affinity of CTCF binding sites, can thereby be used to both influence the number of and length of inter-TAD loops. In turn, both the number and length aspects of extruded loops may be exploited for the regulation of genome-associated functions (see next section).

The mechanistic underpinnings of our model remain to be determined. The function of TAD boundaries as sites for Cohesin release may appear at odds with reports that CTCF competes with the WAPL release factor for binding to Cohesin, thereby stabilizing the DNA-association of the stalled loop extrusion machinery.[74–76,78] Yet, similar to Cohesin and CTCF, WAPL has been found to associate with chromatin in human interphase cells.[90] Moreover, WAPL ChIP-seq experiments that focussed on the mouse *Igh* locus revealed a mostly focal overlap with CTCF binding sites.[58] We therefore envision a mechanism whereby competition between CTCF-mediated stabilization and WAPL-mediated release are both enriched at TAD boundaries. Away from TAD boundaries, constant numbers of Cohesin molecules will be removed by a limited pool of DNA-bound release-factors as well (Figure 3C). Despite the stabilizing impact of CTCF on Cohesin, the enriched presence of WAPL at TAD boundaries will result in the accelerated dissociation as compared to elsewhere in the genome. The validity of our model remains to be determined, including if WAPL indeed achieves accelerated release at TAD boundaries, how the density of WAPL at TAD boundaries compares to sites elsewhere in the genome, what is stoichiometry of WAPL relative to CTCF molecules at boundaries and if release away from boundaries is similarly achieved by WAPL. Particularly important in this respect will be to identify the mechanisms whereby WAPL is recruited to the chromatin and how its enrichment at CTCF binding sites is achieved, including if this is mediated through association with CTCF, Cohesin and/or other unknown factors. In the latter case, this could open up further possibilities for site-specific fine-tuning between stabilization and release of Cohesin and thus the regulation of the number and length of boundary-spanning loops.

In summary, we propose a model whereby TAD boundaries have an elevated capacity to reduce the number of boundary-spanning loops. But due to the release of Cohesin away from TAD boundaries, at a fixed rate over distance, the number of molecules that read through the boundary directly determines the maximum length of inter-TAD loops that can be formed as well.

## 5 | CAN LOOP EXTRUSION STALLING BE USED TO MODULATE EP-LOOPS AND OTHER GENOME-ASSOCIATED FUNCTIONS?

Our model, where the number of boundary-spanning loops determines the number of inter-TAD loops that cover a certain distance and the

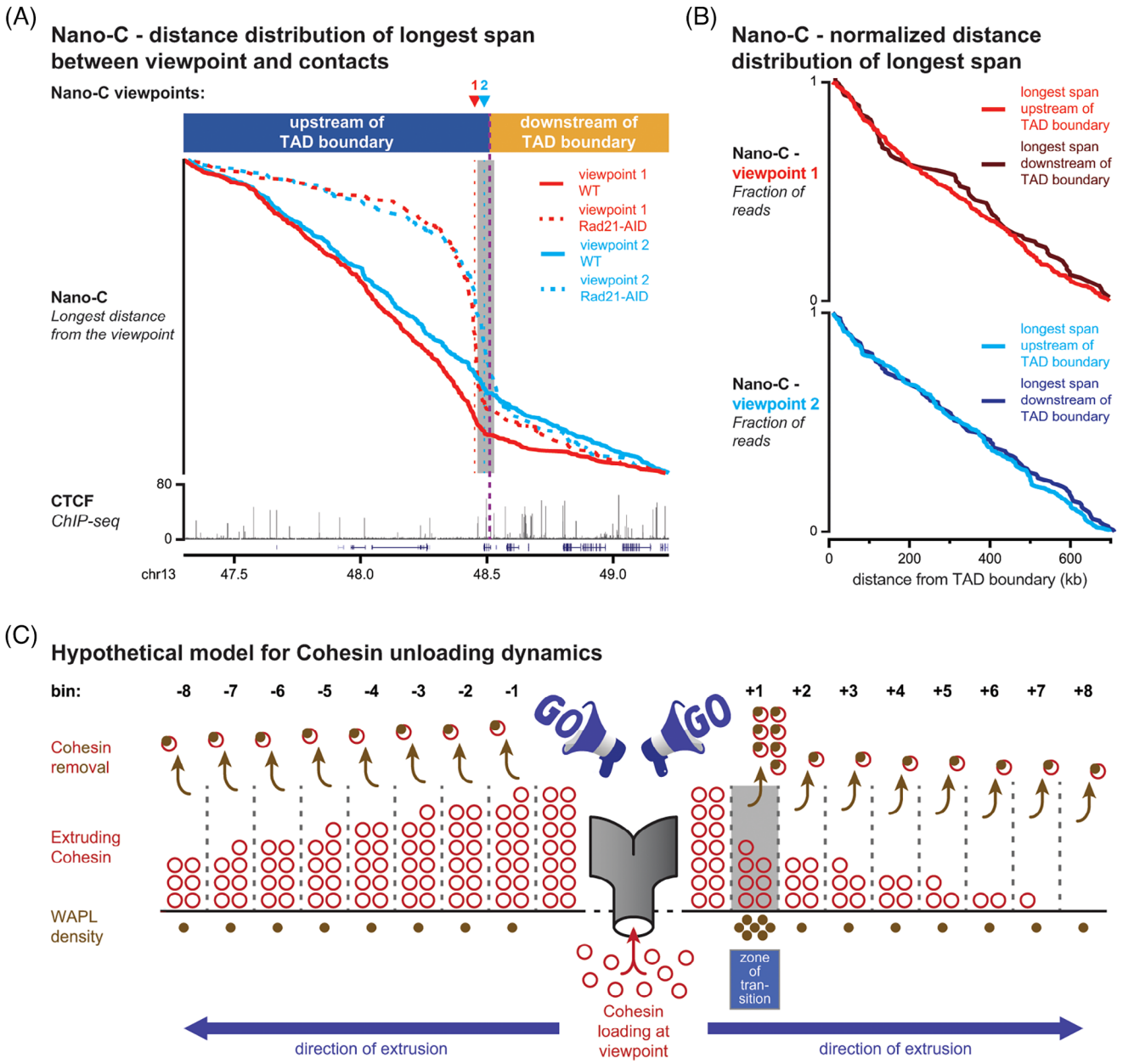


**FIGURE 3** The analysis of the longest span in multicontacts reveals that loop length is not reduced after boundary read-through. (A) Distance distribution of the longest span between the viewpoint and contacts for two viewpoints in the two neighboring TADs, either in normal cells (solid lines) or in cells without active loop extrusion (dashed lines). Reanalyzed data from viewpoints depicted in Figure 2. The TAD boundary is indicated with the purple dashed line, with the extent of the zone of transition highlighted by the gray bar. Position of the viewpoints is indicated with arrowheads (top) and dashed hairlines. Binding of CTCF (ChIP-seq) is depicted below. Original data from Chang et al.[56] (B) Normalized distance distribution from the TAD boundary for the longest span and the viewpoints from panel (A). Interactions upstream (lighter shaded lines) and downstream (darker shaded lines) are indicated separately and limited to the first 700 kb from the boundary. The total fraction of multicontacts is set to 1. Despite different numbers of loops that are present up- and downstream of the boundaries (see panel A), the decrease in distance is linear for extruded loops on both sides of the boundary. The linear shape of the curve indicates a constant rate of Cohesin dissociation within genomic intervals of equal size. (C) Hypothetical model for the release of Cohesin, relative to a fixed loading site. Extrusion in the up- and downstream directions is visualized independently. The amount of removed and remaining Cohesin is indicated for genomic intervals of equal size and at increasing distance from the loading site (−1 to −8 and +1 to +8). The amount of WAPL within a zone of transition is abundant, resulting in a large fraction of Cohesin being removed. Elsewhere in the genome, WAPL amounts are limited and the rate of Cohesin removal is constant. The maximum loop length is attained when no chromatin-associated Cohesin remains.

maximum length of those loops, can be exploited to influence biological processes. Importantly, if Cohesin is removed at a fixed rate, this extends to the regulation of intra-TAD loop distribution as well (see Figure 3B).

For example, the activity of Sonic hedgehog (*Shh*) in the zone of polarizing activity (ZPA) of the limb bud is regulated by a long-range intra-TAD enhancer that is 1-Mb upstream of the *Shh* promoter. Activity of the *Shh* promoter in the ZPA is only observed in a small fraction of cells though,[91] suggesting that the EP-loop is not formed in all cells. Studies that combined imaging with Hi-C/5C (Carbon-Copy Chromosome Conformation Capture) showed that the *Shh* enhancer and promoter were in close spatial proximity in the ZPA, which was promoted by the surrounding TAD that was in a compacted configuration.[92] Whereas the distance between the enhancer and promoter was only mildly increased upon CTCF removal, a nearly complete loss of proximity was observed in the absence of a functioning Cohesin complex.[39] These observations can be explained by our model whereby large numbers of short-range loops create a compacted intra-TAD organization, yet only a few Cohesin molecules achieve extrusion of the entire 1-Mb EP-loop. A similar distance effect was observed when the human $\beta$-globin locus control region (LCR; a super-enhancer) was ectopically integrated in both orientations into a gene-dense region in the mouse genome.[93] The LCR, including a strong CTCF binding site at one side, activated genes both in an orientation and distance-dependent manner over a maximum distance of 150 kb, suggesting that fewer loops could be formed when distance increased. Although generally weaker, genes across the CTCF binding site could be activated as well, suggesting that read-through could result in productive EP-loop formation.[93] More recently, this mechanism was studied in a more systematic manner, by integrating an enhancer at a large number of positions relative to a fixed promoter within the same and otherwise regulatory-neutral TAD.[94] Here, in a window of approximately 10–150 kb from the promoter, a strong and mostly linear relationship was observed between genomic distance and reporter gene activity. This study suggests as well that progressively fewer EP-loops are formed over distance. Addition of a CTCF site in-between the promoter and enhancer caused a strong decrease in the transcriptional output, with a further decrease of the remaining activity over a smaller distance.[94] This result is further in line with our model, whereby sites for loop extrusion-stalling influence both the number and span of productive EP-loops.

Loop extrusion has been implicated in other genome-associated processes as well. One such example is the CTCF-directed regulation of alternative splicing.[95,96] The binding of CTCF within a gene body creates DNA loops that promote the inclusion of introns or alternative exons. This can be explained by interference between Cohesin and RNA polymerase II, whereby the accumulation of the loop extrusion machinery causes pausing of the polymerase elongation rate.[95,97,98] In this case, it can be envisioned that the modulation of loop extrusion read-through influences the stalling of RNA polymerase II and subsequently the rate of alternative splicing. Support for this model may be found in cells with CTCF haploinsufficiency, which display a considerable degree of alternative splicing changes.[99] Another involvement of loop extrusion blocking and read-through is found in the repair of DNA double-strand breaks (DSBs).[57] Upon DSB induction, the Cohesin complex becomes fixed at both sides of the break, thereby inducing a process of divergent one-sided loop extrusion away from the DNA lesion. Through an association of the ATM kinase with the extruding Cohesin complex, this allows a rapid deposition of the $\gamma$H2AX histone modification within large genomic intervals. Functionally, this "scanning" mechanism is similar to the formation of a "stripe" by super-enhancers (Figure 1D).[31,100] The resulting $\gamma$H2AX intervals correlate with TADs and are explained by stalling of the DSB-anchored one-sided loop extrusion by CTCF at TAD boundaries.[57,101] A recent single-cell chromatin profiling study revealed that in a subset of cells, the domains of $\gamma$H2AX can extend across TAD boundaries, indicating a read-through of the boundary by the ATM-associated Cohesin complex.[102] The subsequent span of the domain in the neighboring TADs is more variable, suggesting a progressive removal of Cohesin from the chromatin after the TAD boundary. If this read-through has a biological function, for instance for the improvement of DNA repair outcomes, or rather is a reflection of the permeability of TAD boundaries remains to be determined.

## 6 | CONCLUSIONS AND OUTLOOK

TAD boundaries can regulate EP-loop formation by stalling the extruding Cohesin complex. Here, we have discussed recent evidence that such boundaries are permeable, and we have introduced a model where boundaries can modulate both the number and maximum distance of inter-TAD loops (Figure 3C). Moreover, we highlighted how permeable TAD boundaries may be used to regulate various biological processes.

A major remaining question is if the permeability of TAD boundaries can be regulated, for instance for the modulation of cell type-specific transcriptional programs. The presence of a regulatory mechanism for loop extrusion stalling within the genome can be envisioned, whereby individual sites of stalling can be gained or lost in a cell-type-specific manner. An obvious candidate for such a regulatory mechanism is DNA methylation, whose presence within the CTCF binding motif or the surroundings prevents binding.[17,103–105] Indeed, protocadherin promoter choice and associated CTCF binding is directly determined by differential DNA methylation.[106] The effect of differential CTCF binding may be supplemented with other differential sites of stalling, including cell-type-specific accumulations of (paused) RNA polymerase II (i.e., promoters and enhancers).[35–37,107] A similar mechanism could be envisioned in evolution as well, where reorganization of sites for Cohesin stalling may permit a fine-tuning of gene expression.[13,62,108] More systematic comparisons of TAD boundary permeability in different cell types and species will be needed to determine if modulation of boundaries at the level of DNA sequence or DNA methylation is commonly employed. Moreover, the potential influence of sequence-encoded cues for the differential amounts of Cohesin loading and release should be included as well.[34,88,90]

A second remaining question is related to the observation that the fusion of neighboring TADs frequently requires the removal of multiple

sites of CTCF binding.[64–67] Clustering of sites for the stalling of loop extrusion creates resilience against the perturbations of individual CTCF sites but also increases the size of the genomic intervals where structural variation can exert its effect. Changes to chromatin looping are commonly linked to human disease, with mutations and DNA methylation changes frequently observed at CTCF binding sites in cancer cells.[19,109–112] If these changes affect a single site of Cohesin stalling, our model predicts that changes in gene expression can be moderate. Additional studies, focussing on more minor changes in transcription will be required to determine the importance and prevalence of reorganized loop extrusion stalling within the zones of transition that surround TAD boundaries.

## AUTHOR CONTRIBUTIONS

Li-Hsin Chang and Daan Noordermeer conceived the hypothesis, researched the literature and wrote the manuscript.

## ACKNOWLEDGMENTS

We thank the members of the James Davies (University of Oxford) and Noordermeer (Université Paris-Saclay) teams for useful discussion. L.-H. C. acknowledges funding from the Blood and Transplant Research Unit in Precision Cellular Therapeutics. D. N. acknowledges funding from the Agence Nationale de la Recherche (Grants ANR-21-CE12-0034, ANR-22-CE12-0016, and ANR-22-CE14-0021).

## CONFLICT OF INTEREST STATEMENT

The authors declare no conflicts of interest.

## DATA AVAILABILITY STATEMENT

Data sharing is not applicable to this article as no new data were created for this manuscript. The original data used for the reanalysis are available, without restrictions, from https://data.mendeley.com/datasets/g7b4z8957z/4.

## ORCID

*Li-Hsin Chang* https://orcid.org/0009-0002-8193-8203
*Daan Noordermeer* https://orcid.org/0000-0002-9296-7002

## REFERENCES

1. Tolhuis, B., Palstra, R.-J., Splinter, E., Grosveld, F., & De Laat, W. (2002). Looping and interaction between hypersensitive sites in the active beta-globin locus. *Molecular Cell*, *10*, 1453–1465.
2. Sanyal, A., Lajoie, B. R., Jain, G., & Dekker, J. (2012). The long-range interaction landscape of gene promoters. *Nature*, *489*, 109–113.
3. Shen, Y., Yue, F., Mccleary, D. F., Ye, Z., Edsall, L., Kuan, S., Wagner, U., Dixon, J., Lee, L., Lobanenkov, V. V., & Ren, B. (2012). A map of the cis-regulatory sequences in the mouse genome. *Nature*, *488*, 116–120.
4. Long, H. K., Osterwalder, M., Welsh, I. C., Hansen, K., Davies, J. O. J., Liu, Y. E., Koska, M., Adams, A. T., Aho, R., Arora, N., Ikeda, K., Williams, R. M., Sauka-Spengler, T., Porteus, M. H., Mohun, T., Dickel, D. E., Swigut, T., Hughes, J. R., Higgs, D. R., … Wysocka, J. (2020). Loss of extreme long-range enhancers in human neural crest drives a craniofacial disorder. *Cell Stem Cell*, *27*, 765–783.e14.
5. Lobanenkov, V. V., Nicolas, R. H., Adler, V. V., Paterson, H., Klenova, E. M., Polotskaja, A. V., & Goodwin, G. H. (1990). A novel sequence-specific DNA binding protein which interacts with three regularly spaced direct repeats of the CCCTC-motif in the 5'-flanking sequence of the chicken c-myc gene. *Oncogene*, *5*, 1743–1753.
6. Bell, A. C., West, A. G., & Felsenfeld, G. (1999). The protein CTCF is required for the enhancer blocking activity of vertebrate insulators. *Cell*, *98*, 387–396.
7. Kim, T. H., Abdullaev, Z. K., Smith, A. D., Ching, K. A., Loukinov, D. I., Green, R. D., Zhang, M. Q., Lobanenkov, V. V., & Ren, B. (2007). Analysis of the vertebrate insulator protein CTCF-binding sites in the human genome. *Cell*, *128*, 1231–1245.
8. Dixon, J. R., Selvaraj, S., Yue, F., Kim, A., Li, Y., Shen, Y., Hu, M., Liu, J. S., & Ren, B. (2012). Topological domains in mammalian genomes identified by analysis of chromatin interactions. *Nature*, *485*, 376–380.
9. Nora, E. P., Lajoie, B. R., Schulz, E. G., Giorgetti, L., Okamoto, I., Servant, N., Piolot, T., Van Berkum, N. L., Meisig, J., Sedat, J., Gribnau, J., Barillot, E., Blüthgen, N., Dekker, J., & Heard, E. (2012). Spatial partitioning of the regulatory landscape of the X-inactivation centre. *Nature*, *485*, 381–385.
10. Rao, S. S. P., Huntley, M. H., Durand, N. C., Stamenova, E. K., Bochkov, I. D., Robinson, J. T., Sanborn, A. L., Machol, I., Omer, A. D., Lander, E. S., & Aiden, E. L. (2014). A 3D map of the human genome at kilobase resolution reveals principles of chromatin looping. *Cell*, *159*, 1665–1680.
11. De Wit, E., Vos, E. S. M., Holwerda, S. J. B., Valdes-Quezada, C., Verstegen, M., Teunissen, H., Splinter, E., Wijchers, P. J., Krijger, P. H. L., & De Laat, W. (2015). CTCF binding polarity determines chromatin looping. *Molecular Cell*, *60*, 676–684.
12. Guo, Y., Xu, Q., Canzio, D., Shou, J., Li, J., Gorkin, D. U., Jung, I., Wu, H., Zhai, Y., Tang, Y., Lu, Y., Wu, Y., Jia, Z., Li, W., Zhang, M. Q., Ren, B., Krainer, A. R., Maniatis, T., & Wu, Q. (2015). CRISPR inversion of CTCF sites alters genome topology and enhancer/promoter function. *Cell*, *162*, 900–910.
13. Vietri Rudan, M., Barrington, C., Henderson, S., Ernst, C., Odom, D. T., Tanay, A., & Hadjur, S. (2015). Comparative Hi-C reveals that CTCF underlies evolution of chromosomal domain architecture. *Cell Reports*, *10*, 1297–1309.
14. Nora, E. P., Dekker, J., & Heard, E. (2013). Segmental folding of chromosomes: A basis for structural and regulatory chromosomal neighborhoods? *BioEssays*, *35*, 818–828.
15. Dowen, J. M., Fan, Z. P., Hnisz, D., Ren, G., Abraham, B. J., Zhang, L. N., Weintraub, A. S., Schuijers, J., Lee, T. I., Zhao, K., & Young, R. A. (2014). Control of cell identity genes occurs in insulated neighborhoods in mammalian chromosomes. *Cell*, *159*, 374–387.
16. Chang, L.-H., Ghosh, S., & Noordermeer, D. (2020). TADs and their borders: Free movement or building a wall? *Journal of Molecular Biology*, *432*, 643–652.
17. Andrey, G., Montavon, T., Mascrez, B., Gonzalez, F., Noordermeer, D., Leleu, M., Trono, D., Spitz, F., & Duboule, D. (2013). A switch between topological domains underlies HoxD genes collinearity in mouse limbs. *Science*, *340*, 1195.
18. Lupiáñez, D. G., Kraft, K., Heinrich, V., Krawitz, P., Brancati, F., Klopocki, E., Horn, D., Kayserili, H., Opitz, J. M., Laxova, R., Santos-Simarro, F., Gilbert-Dussardier, B., Wittler, L., Borschiwer, M., Haas, S. A., Osterwalder, M., Franke, M., Timmermann, B., Hecht, J., … Mundlos, S. (2015). Disruptions of topological chromatin domains cause pathogenic rewiring of gene-enhancer interactions. *Cell*, *161*, 1012–1025.
19. Flavahan, W. A., Drier, Y., Liau, B. B., Gillespie, S. M., Venteicher, A. S., Stemmer-Rachamimov, A. O., Suvà, M. L., & Bernstein, B. E. (2016). Insulator dysfunction and oncogene activation in IDH mutant gliomas. *Nature*, *529*, 110–114.
20. Llères, D., Moindrot, B., Pathak, R., Piras, V., Matelot, M., Pignard, B., Marchand, A., Poncelet, M., Perrin, A., Tellier, V., Feil, R., & Noordermeer, D. (2019). CTCF modulates allele-specific sub-TAD

organization and imprinted gene activity at the mouse Dlk1-Dio3 and Igf2-H19 domains. *Genome Biology*, *20*, 272.
21. Rahme, G. J., Javed, N. M., Puorro, K. L., Xin, S., Hovestadt, V., Johnstone, S. E., & Bernstein, B. E. (2023). Modeling epigenetic lesions that cause gliomas. *Cell*, *186*, 3674–3685.e14.
22. Rajderkar, S., Barozzi, I., Zhu, Y., Hu, R., Zhang, Y., Li, B., Alcaina Caro, A., Fukuda-Yuzawa, Y., Kelman, G., Akeza, A., Blow, M. J., Pham, Q., Harrington, A. N., Godoy, J., Meky, E. M., Von Maydell, K., Hunter, R. D., Akiyama, J. A., Novak, C. S., … Pennacchio, L. A. (2023). Topologically Associating Domain boundaries are required for normal genome function. *Communications Biology*, *6*, 435.
23. Sanborn, A. L., Rao, S. S. P., Huang, S.-C., Durand, N. C., Huntley, M. H., Jewett, A. I., Bochkov, I. D., Chinnappan, D., Cutkosky, A., Li, J., Geeting, K. P., Gnirke, A., Melnikov, A., Mckenna, D., Stamenova, E. K., Lander, E. S., & Aiden, E. L. (2015). Chromatin extrusion explains key features of loop and domain formation in wild-type and engineered genomes. *PNAS*, *112*, E6456–E6465.
24. Fudenberg, G., Imakaev, M., Lu, C., Goloborodko, A., Abdennur, N., & Mirny, L. A. (2016). Formation of chromosomal domains by loop extrusion. *Cell Reports*, *15*, 2038–2049.
25. Rao, S. S. P., Huang, S.-C., Glenn St Hilaire, B., Engreitz, J. M., Perez, E. M., Kieffer-Kwon, K.-R., Sanborn, A. L., Johnstone, S. E., Bascom, G. D., Bochkov, I. D., Huang, X., Shamim, M. S., Shin, J., Turner, D., Ye, Z., Omer, A. D., Robinson, J. T., Schlick, T., Bernstein, B. E., … Aiden, E. L. (2017). Cohesin loss eliminates all loop domains. *Cell*, *171*, 305–320.e24.
26. Schwarzer, W., Abdennur, N., Goloborodko, A., Pekowska, A., Fudenberg, G., Loe-Mie, Y., Fonseca, N. A., Huber, W., Haering, C. H., Mirny, L., & Spitz, F. (2017). Two independent modes of chromatin organization revealed by cohesin removal. *Nature*, *551*, 51–56.
27. Davidson, I. F., Bauer, B., Goetz, D., Tang, W., Wutz, G., & Peters, J.-M. (2019). DNA loop extrusion by human cohesin. *Science*, *366*, 1338–1345.
28. Kim, Y., Shi, Z., Zhang, H., Finkelstein, I. J., & Yu, H. (2019). Human cohesin compacts DNA by loop extrusion. *Science*, *366*, 1345–1349.
29. Golfier, S., Quail, T., Kimura, H., & Brugués, J. (2020). Cohesin and condensin extrude DNA loops in a cell cycle-dependent manner. *Elife*, *9*, e53885.
30. Dekker, C., Haering, C. H., Peters, J.-M., & Rowland, B. D. (2023). How do molecular motors fold the genome? *Science*, *382*, 646–648.
31. Vian, L., Pękowska, A., Rao, S. S. P., Kieffer-Kwon, K.-R., Jung, S., Baranello, L., Huang, S.-C., El Khattabi, L., Dose, M., Pruett, N., Sanborn, A. L., Canela, A., Maman, Y., Oksanen, A., Resch, W., Li, X., Lee, B., Kovalchuk, A. L., Tang, Z., … Casellas, R. (2018). The energetics and physiological impact of cohesin extrusion. *Cell*, *173*, 1165–1178.e20.
32. Barrington, C., Georgopoulou, D., Pezic, D., Varsally, W., Herrero, J., & Hadjur, S. (2019). Enhancer accessibility and CTCF occupancy underlie asymmetric TAD architecture and cell type specific genome topology. *Nature Communications*, *10*, 2908.
33. Hsieh, T.-H. S., Cattoglio, C., Slobodyanyuk, E., Hansen, A. S., Rando, O. J., Tjian, R., & Darzacq, X. (2020). Resolving the 3D landscape of transcription-linked mammalian chromatin folding. *Molecular Cell*, *78*, 539–553.e8.
34. Zhu, Y., Denholtz, M., Lu, H., & Murre, C. (2021). Calcium signaling instructs NIPBL recruitment at active enhancers and promoters via distinct mechanisms to reconstruct genome compartmentalization. *Genes & Development*, *35*, 65–81.
35. Barshad, G., Lewis, J. J., Chivu, A. G., Abuhashem, A., Krietenstein, N., Rice, E. J., Ma, Y., Wang, Z., Rando, O. J., Hadjantonakis, A.-K., & Danko, C. G. (2023). RNA polymerase II dynamics shape enhancer-promoter interactions. *Nature Genetics*, *55*, 1370–1380.
36. Zhang, S., Übelmesser, N., Barbieri, M., & Papantonis, A. (2023). Enhancer-promoter contact formation requires RNAPII and antagonizes loop extrusion. *Nature Genetics*, *55*, 832–840.
37. Noordermeer, D. (2023). RNA Pol II enters the ring of cohesin-mediated loop extrusion. *Nature Genetics*, *55*, 1256–1258.
38. Calderon, L., Weiss, F. D., Beagan, J. A., Oliveira, M. S., Georgieva, R., Wang, Y.-F., Carroll, T. S., Dharmalingam, G., Gong, W., Tossell, K., De Paola, V., Whilding, C., Ungless, M. A., Fisher, A. G., Phillips-Cremins, J. E., & Merkenschlager, M. (2022). Cohesin-dependence of neuronal gene expression relates to chromatin loop length. *Elife*, *11*, e76539.
39. Kane, L., Williamson, I., Flyamer, I. M., Kumar, Y., Hill, R. E., Lettice, L. A., & Bickmore, W. A. (2022). Cohesin is required for long-range enhancer action at the Shh locus. *Nature Structural & Molecular Biology*, *29*, 891–897.
40. Schmitt, A. D., Hu, M., Jung, I., Xu, Z., Qiu, Y., Tan, C. L., Li, Y., Lin, S., Lin, Y., Barr, C. L., & Ren, B. (2016). A compendium of chromatin contact maps reveals spatially active regions in the human genome. *Cell Reports*, *17*, 2042–2059.
41. Schuijers, J., Manteiga, J. C., Weintraub, A. S., Day, D. S., Zamudio, A. V., Hnisz, D., Lee, T. I., & Young, R. A. (2018). Transcriptional dysregulation of MYC reveals common enhancer-docking mechanism. *Cell Reports*, *23*, 349–360.
42. Kueng, S., Hegemann, B., Peters, B. H., Lipp, J. J., Schleiffer, A., Mechtler, K., & Peters, J.-M. (2006). Wapl controls the dynamic association of cohesin with chromatin. *Cell*, *127*, 955–967.
43. Tedeschi, A., Wutz, G., Huet, S., Jaritz, M., Wuensche, A., Schirghuber, E., Davidson, I. F., Tang, W., Cisneros, D. A., Bhaskara, V., Nishiyama, T., Vaziri, A., A., Ellenberg, J., & Peters, J.-M. (2013). Wapl is an essential regulator of chromatin structure and chromosome segregation. *Nature*, *501*, 564–568.
44. Haarhuis, J. H. I., Van Der Weide, R. H., Blomen, V. A., Yáñez-Cuna, J. O., Amendola, M., Van Ruiten, M. S., Krijger, P. H. L., Teunissen, H., Medema, R. H., Van Steensel, B., Brummelkamp, T. R., De Wit, E., & Rowland, B. D. (2017). The cohesin release factor WAPL restricts chromatin loop extension. *Cell*, *169*, 693–707.e14.
45. Wutz, G., Várnai, C., Nagasaka, K., Cisneros, D. A., Stocsits, R. R., Tang, W., Schoenfelder, S., Jessberger, G., Muhar, M., Hossain, M. J., Walther, N., Koch, B., Kueblbeck, M., Ellenberg, J., Zuber, J., Fraser, P., & Peters, J.-M. (2017). Topologically Associating Domains and chromatin loops depend on cohesin and are regulated by CTCF, WAPL, and PDS5 proteins. *The EMBO Journal*, *36*, 3573–3599.
46. Gabriele, M., Brandão, H. B., Grosse-Holz, S., Jha, A., Dailey, G. M., Cattoglio, C., Hsieh, T.-H. S., Mirny, L., Zechner, C., & Hansen, A. S. (2022). Dynamics of CTCF- and cohesin-mediated chromatin looping revealed by live-cell imaging. *Science*, *376*, 496–501.
47. Mach, P., Kos, P. I., Zhan, Y., Cramard, J., Gaudin, S., Tünnermann, J., Marchi, E., Eglinger, J., Zuin, J., Kryzhanovska, M., Smallwood, S., Gelman, L., Roth, G., Nora, E. P., Tiana, G., & Giorgetti, L. (2022). Cohesin and CTCF control the dynamics of chromosome folding. *Nature Genetics*, *54*, 1907–1918.
48. Da Costa-Nunes, J. A., & Noordermeer, D. (2023). TADs: Dynamic structures to create stable regulatory functions. *Current Opinion in Structural Biology*, *81*, 102622.
49. Hafner, A., & Boettiger, A. (2023). The spatial organization of transcriptional control. *Nature Reviews Genetics*, *24*, 53–68.
50. Nagano, T., Lubling, Y., Stevens, T. J., Schoenfelder, S., Yaffe, E., Dean, W., Laue, E. D., Tanay, A., & Fraser, P. (2013). Single-cell Hi-C reveals cell-to-cell variability in chromosome structure. *Nature*, *502*, 59–64.
51. Bintu, B., Mateo, L. J., Su, J.-H., Sinnott-Armstrong, N. A., Parker, M., Kinrot, S., Yamaya, K., Boettiger, A. N., & Zhuang, X. (2018). Super-resolution chromatin tracing reveals domains and cooperative interactions in single cells. *Science*, *362*, eaau1783.
52. Hansen, A. S., Cattoglio, C., Darzacq, X., & Tjian, R. (2018). Recent evidence that TADs and chromatin loops are dynamic structures. *Nucleus*, *9*, 20–32.
53. Oudelaar, A. M., Davies, J. O. J., Hanssen, L. L. P., Telenius, J. M., Schwessinger, R., Liu, Y., Brown, J. M., Downes, D. J., Chiariello, A. M., Bianco, S., Nicodemi, M., Buckle, V. J., Dekker, J., Higgs, D. R.,

& Hughes, J. R. (2018). Single-allele chromatin interactions identify regulatory hubs in dynamic compartmentalized domains. *Nature Genetics*, *50*, 1744–1751.
54. Luppino, J. M., Park, D. S., Nguyen, S. C., Lan, Y., Xu, Z., Yunker, R., & Joyce, E. F. (2020). Cohesin promotes stochastic domain intermingling to ensure proper regulation of boundary-proximal genes. *Nature Genetics*, *52*, 840–848.
55. Szabo, Q., Donjon, A., Jerković, I., Papadopoulos, G. L., Cheutin, T., Bonev, B., Nora, E. P., Bruneau, B. G., Bantignies, F., & Cavalli, G. (2020). Regulation of single-cell genome organization into TADs and chromatin nanodomains. *Nature Genetics*, *52*, 1151–1157.
56. Chang, L.-H., Ghosh, S., Papale, A., Luppino, J. M., Miranda, M., Piras, V., Degrouard, J., Edouard, J., Poncelet, M., Lecouvreur, N., Bloyer, S., Leforestier, A., Joyce, E. F., Holcman, D., & Noordermeer, D. (2023). Multi-feature clustering of CTCF binding creates robustness for loop extrusion blocking and Topologically Associating Domain boundaries. *Nature Communications*, *14*, 5615.
57. Arnould, C., Rocher, V., Finoux, A.-L., Clouaire, T., Li, K., Zhou, F., Caron, P., Mangeot, P. E., Ricci, E. P., Mourad, R., Haber, J. E., Noordermeer, D., & Legube, G. (2021). Loop extrusion as a mechanism for formation of DNA damage repair foci. *Nature*, *590*, 660–665.
58. Dai, H.-Q., Hu, H., Lou, J., Ye, A. Y., Ba, Z., Zhang, X., Zhang, Y., Zhao, L., Yoon, H. S., Chapdelaine-Williams, A. M., Kyritsis, N., Chen, H., Johnson, K., Lin, S., Conte, A., Casellas, R., Lee, C.-S., & Alt, F. W. (2021). Loop extrusion mediates physiological Igh locus contraction for RAG scanning. *Nature*, *590*, 338–343.
59. Emerson, D. J., Zhao, P. A., Cook, A. L., Barnett, R. J., Klein, K. N., Saulebekova, D., Ge, C., Zhou, L., Simandi, Z., Minsk, M. K., Titus, K. R., Wang, W., Gong, W., Zhang, D., Yang, L., Venev, S. V., Gibcus, J. H., Yang, H., Sasaki, T., … Phillips-Cremins, J. E. (2022). Cohesin-mediated loop anchors confine the locations of human replication origins. *Nature*, *606*, 812–819.
60. Phillips-Cremins, J. E., & Corces, V. G. (2013). Chromatin insulators: linking genome organization to cellular function. *Molecular Cell*, *50*, 461–474.
61. Madani Tonekaboni, S. A., Mazrooei, P., Kofia, V., Haibe-Kains, B., & Lupien, M. (2019). Identifying clusters of cis-regulatory elements underpinning TAD structures and lineage-specific regulatory networks. *Genome Research*, *29*, 1733–1743.
62. Kentepozidou, E., Aitken, S. J., Feig, C., Stefflova, K., Ibarra-Soria, X., Odom, D. T., Roller, M., & Flicek, P. (2020). Clustered CTCF binding is an evolutionary mechanism to maintain Topologically Associating Domains. *Genome Biology*, *21*, 5.
63. Nanni, L., Ceri, S., & Logie, C. (2020). Spatial patterns of CTCF sites define the anatomy of TADs and their boundaries. *Genome Biology*, *21*, 197.
64. Despang, A., Schöpflin, R., Franke, M., Ali, S., Jerković, I., Paliou, C., Chan, W.-L., Timmermann, B., Wittler, L., Vingron, M., Mundlos, S., & Ibrahim, D. M. (2019). Functional dissection of the Sox9-Kcnj2 locus identifies nonessential and instructive roles of TAD architecture. *Nature Genetics*, *51*, 1263–1271.
65. Paliou, C., Guckelberger, P., Schöpflin, R., Heinrich, V., Esposito, A., Chiariello, A. M., Bianco, S., Annunziatella, C., Helmuth, J., Haas, S., Jerković, I., Brieske, N., Wittler, L., Timmermann, B., Nicodemi, M., Vingron, M., Mundlos, S., & Andrey, G. (2019). Preformed chromatin topology assists transcriptional robustness of Shh during limb development. *PNAS*, *116*, 12390–12399.
66. Williamson, I., Kane, L., Devenney, P. S., Flyamer, I. M., Anderson, E., Kilanowski, F., Hill, R. E., Bickmore, W. A., & Lettice, L. A. (2019). Developmentally regulated Shh expression is robust to TAD perturbations. *Development (Cambridge, England)*, *146*, dev179523.
67. Anania, C., Acemel, R. D., Jedamzick, J., Bolondi, A., Cova, G., Brieske, N., Kühn, R., Wittler, L., Real, F. M., & Lupiáñez, D. G. (2022). In vivo dissection of a clustered-CTCF domain boundary reveals developmental principles of regulatory insulation. *Nature Genetics*, *54*, 1026–1036.
68. Kim, K. L., Rahme, G. J., Goel, V. Y., El Farran, C. A., Hansen, A. S., & Bernstein, B. E. (2024). Dissection of a CTCF topological boundary uncovers principles of enhancer-oncogene regulation. *Molecular Cell*, *84*, 1365–1376.e7.
69. Huang, H., Zhu, Q., Jussila, A., Han, Y., Bintu, B., Kern, C., Conte, M., Zhang, Y., Bianco, S., Chiariello, A. M., Yu, M., Hu, R., Tastemel, M., Juric, I., Hu, M., Nicodemi, M., Zhuang, X., & Ren, B. (2021). CTCF mediates dosage- and sequence-context-dependent transcriptional insulation by forming local chromatin domains. *Nature Genetics*, *53*, 1064–1074.
70. Chakraborty, S., Kopitchinski, N., Zuo, Z., Eraso, A., Awasthi, P., Chari, R., Mitra, A., Tobias, I. C., Moorthy, S. D., Dale, R. K., Mitchell, J. A., Petros, T. J., & Rocha, P. P. (2023). Enhancer-promoter interactions can bypass CTCF-mediated boundaries and contribute to phenotypic robustness. *Nature Genetics*, *55*, 280–290.
71. Hansen, A. S., Pustova, I., Cattoglio, C., Tjian, R., & Darzacq, X. (2017). CTCF and cohesin regulate chromatin loop stability with distinct dynamics. *Elife*, *6*, e25776.
72. Holzmann, J., Politi, A. Z., Nagasaka, K., Hantsche-Grininger, M., Walther, N., Koch, B., Fuchs, J., Dürnberger, G., Tang, W., Ladurner, R., Stocsits, R. R., Busslinger, G. A., Novák, B., Mechtler, K., Davidson, I. F., Ellenberg, J., & Peters, J.-M. (2019). Absolute quantification of cohesin, CTCF and their regulators in human cells. *Elife*, *8*, e46269.
73. Cattoglio, C., Pustova, I., Walther, N., Ho, J. J., Hantsche-Grininger, M., Inouye, C. J., Hossain, M. J., Dailey, G. M., Ellenberg, J., Darzacq, X., Tjian, R., & Hansen, A. S. (2019). Determining cellular CTCF and cohesin abundances to constrain 3D genome models. *Elife*, *8*, e40164.
74. Li, Y., Haarhuis, J. H. I., Sedeño Cacciatore, Á., Oldenkamp, R., Van Ruiten, M. S., Willems, L., Teunissen, H., Muir, K. W., De Wit, E., Rowland, B. D., & Panne, D. (2020). The structural basis for cohesin-CTCF-anchored loops. *Nature*, *578*, 472–476.
75. Nora, E. P., Caccianini, L., Fudenberg, G., So, K., Kameswaran, V., Nagle, A., Uebersohn, A., Hajj, B., Saux, A. L., Coulon, A., Mirny, L. A., Pollard, K. S., Dahan, M., & Bruneau, B. G. (2020). Molecular basis of CTCF binding polarity in genome folding. *Nature Communications*, *11*, 5612.
76. Rubio, E. D., Reiss, D. J., Welcsh, P. L., Disteche, C. M., Filippova, G. N., Baliga, N. S., Aebersold, R., Ranish, J. A., & Krumm, A. (2008). CTCF physically links cohesin to chromatin. *PNAS*, *105*, 8309–8314.
77. Kojic, A., Cuadrado, A., De Koninck, M., Giménez-Llorente, D., Rodríguez-Corsino, M., Gómez-López, G., Le Dily, F., Marti-Renom, M. A., & Losada, A. (2018). Distinct roles of cohesin-SA1 and cohesin-SA2 in 3D chromosome organization. *Nature Structural & Molecular Biology*, *25*, 496–504.
78. Wutz, G., Ladurner, R., St Hilaire, B. G., Stocsits, R. R., Nagasaka, K., Pignard, B., Sanborn, A., Tang, W., Várnai, C., Ivanov, M. P., Schoenfelder, S., Van Der Lelij, P., Huang, X., Dürnberger, G., Roitinger, E., Mechtler, K., Davidson, I. F., Fraser, P., Lieberman-Aiden, E., & Peters, J.-M. (2020). ESCO1 and CTCF enable formation of long chromatin loops by protecting cohesin(STAG1) from WAPL. *Elife*, *9*, e52091.
79. Luan, J., Xiang, G., Gómez-García, P. A., Tome, J. M., Zhang, Z., Vermunt, M. W., Zhang, H., Huang, A., Keller, C. A., Giardine, B. M., Zhang, Y., Lan, Y., Lis, J. T., Lakadamyali, M., Hardison, R. C., & Blobel, G. A. (2021). Distinct properties and functions of CTCF revealed by a rapidly inducible degron system. *Cell Reports*, *34*, 108783.
80. Van Ruiten, M. S., Van Gent, D., Sedeño Cacciatore, Á., Fauster, A., Willems, L., Hekkelman, M. L., Hoekman, L., Altelaar, M., Haarhuis, J. H. I., Brummelkamp, T. R., De Wit, E., & Rowland, B. D. (2022). The cohesin acetylation cycle controls chromatin loop length through a PDS5A brake mechanism. *Nature Structural & Molecular Biology*, *29*, 586–591.
81. Davidson, I. F., Barth, R., Zaczek, M., Van Der Torre, J., Tang, W., Nagasaka, K., Janissen, R., Kerssemakers, J., Wutz, G., Dekker, C., &

Peters, J.-M. (2023). CTCF is a DNA-tension-dependent barrier to cohesin-mediated loop extrusion. *Nature*, *616*, 822–827.
82. Huber, J., Tanasie, N.-L., Zernia, S., & Stigler, J. (2024). Single-molecule imaging reveals a direct role of CTCF's zinc fingers in SA interaction and cluster-dependent RNA recruitment. *Nucleic Acids Research*, *52*, 6490–6506.
83. Olivares-Chauvet, P., Mukamel, Z., Lifshitz, A., Schwartzman, O., Elkayam, N. O., Lubling, Y., Deikus, G., Sebra, R. P., & Tanay, A. (2016). Capturing pairwise and multi-way chromosomal conformations using chromosomal walks. *Nature*, *540*, 296–300.
84. Zheng, M., Tian, S. Z., Capurso, D., Kim, M., Maurya, R., Lee, B., Piecuch, E., Gong, L., Zhu, J. J., Li, Z., Wong, C. H., Ngan, C. Y., Wang, P., Ruan, X., Wei, C.-L., & Ruan, Y. (2019). Multiplex chromatin interactions with single-molecule precision. *Nature*, *566*, 558–562.
85. Tavares-Cadete, F., Norouzi, D., Dekker, B., Liu, Y., & Dekker, J. (2020). Multi-contact 3C reveals that the human genome during interphase is largely not entangled. *Nature Structural & Molecular Biology*, *27*, 1105–1114.
86. Deshpande, A. S., Ulahannan, N., Pendleton, M., Dai, X., Ly, L., Behr, J. M., Schwenk, S., Liao, W., Augello, M. A., Tyer, C., Rughani, P., Kudman, S., Tian, H., Otis, H. G., Adney, E., Wilkes, D., Mosquera, J. M., Barbieri, C. E., Melnick, A., … Imieliński, M. (2022). Identifying synergistic high-order 3D chromatin conformations from genome-scale nanopore concatemer sequencing. *Nature Biotechnology*, *40*, 1488–1499.
87. Allahyar, A., Vermeulen, C., Bouwman, B. A. M., Krijger, P. H. L., Verstegen, M., Geeven, G., Van Kranenburg, M., Pieterse, M., Straver, R., Haarhuis, J. H. I., Jalink, K., Teunissen, H., Renkens, I. J., Kloosterman, W. P., Rowland, B. D., De Wit, E., De Ridder, J., & De Laat, W. (2018). Enhancer hubs and loop collisions identified from single-allele topologies. *Nature Genetics*, *50*, 1151–1160.
88. Liu, N. Q., Maresca, M., Van Den Brand, T., Braccioli, L., Schijns, M., Teunissen, H., Bruneau, B. G., Nora, E. P., & De Wit, E. (2021). WAPL maintains a cohesin loading cycle to preserve cell-type-specific distal gene regulation. *Nature Genetics*, *53*, 100–109.
89. Noordermeer, D., Chang, L. H., & Ghosh, S. (2023). *Multi-feature clustering of CTCF binding creates robustness for loop extrusion blocking and Topologically Associating Domain boundaries.* Mendeley Data, g7b4z8957z/4. https://data.mendeley.com/datasets/g7b4z8957z/4
90. Gandhi, R., Gillespie, P. J., & Hirano, T. (2006). Human Wapl is a cohesin-binding protein that promotes sister-chromatid resolution in mitotic prophase. *Current Biology*, *16*, 2406–2417.
91. Amano, T., Sagai, T., Tanabe, H., Mizushina, Y., Nakazawa, H., & Shiroishi, T. (2009). Chromosomal dynamics at the Shh locus: Limb bud-specific differential regulation of competence and active transcription. *Developmental Cell*, *16*, 47–57.
92. Williamson, I., Lettice, L. A., Hill, R. E., & Bickmore, W. A. (2016). Shh and ZRS enhancer co-localisation is specific to the zone of polarizing activity. *Development (Cambridge, England)*, *143*, 2994–3001.
93. Noordermeer, D., Branco, M. R., Splinter, E., Klous, P., Van Ijcken, W., Swagemakers, S., Koutsourakis, M., Van Der Spek, P., Pombo, A., & De Laat, W. (2008). Transcription and chromatin organization of a housekeeping gene cluster containing an integrated beta-globin locus control region. *Plos Genetics*, *4*, e1000016.
94. Zuin, J., Roth, G., Zhan, Y., Cramard, J., Redolfi, J., Piskadlo, E., Mach, P., Kryzhanovska, M., Tihanyi, G., Kohler, H., Eder, M., Leemans, C., Van Steensel, B., Meister, P., Smallwood, S., & Giorgetti, L. (2022). Nonlinear control of transcription through enhancer-promoter interactions. *Nature*, *604*, 571–577.
95. Shukla, S., Kavak, E., Gregory, M., Imashimizu, M., Shutinoski, B., Kashlev, M., Oberdoerffer, P., Sandberg, R., & Oberdoerffer, S. (2011). CTCF-promoted RNA polymerase II pausing links DNA methylation to splicing. *Nature*, *479*, 74–79.
96. Ruiz-Velasco, M., Kumar, M., Lai, M. C., Bhat, P., Solis-Pinson, A. B., Reyes, A., Kleinsorg, S., Noh, K. M., Gibson, T. J., & Zaugg, J. B. (2017). CTCF-mediated chromatin loops between promoter and gene body regulate alternative splicing across individuals. *Cell Systems*, *5*, 628–637 e6.
97. Valton, A.-L., Venev, S. V., Mair, B., Khokhar, E. S., Tong, A. H. Y., Usaj, M., Chan, K., Pai, A. A., Moffat, J., & Dekker, J. (2022). A cohesin traffic pattern genetically linked to gene regulation. *Nature Structural & Molecular Biology*, *29*, 1239–1251.
98. Banigan, E. J., Tang, W., Van Den Berg, A. A., Stocsits, R. R., Wutz, G., Brandão, H. B., Busslinger, G. A., Peters, J.-M., & Mirny, L. A. (2023). Transcription shapes 3D chromatin organization by interacting with loop extrusion. *PNAS*, *120*, e2210480120.
99. Alharbi, A. B., Schmitz, U., Marshall, A. D., Vanichkina, D., Nagarajah, R., Vellozzi, M., Wong, J. J., Bailey, C. G., & Rasko, J. E. (2021). Ctcf haploinsufficiency mediates intron retention in a tissue-specific manner. *RNA Biology*, *18*, 93–103.
100. Mirny, L. A. (2021). Loops that mend the genome. *Nature*, *590*, 554–555.
101. Collins, P. L., Purman, C., Porter, S. I., Nganga, V., Saini, A., Hayer, K. E., Gurewitz, G. L., Sleckman, B. P., Bednarski, J. J., Bassing, C. H., & Oltz, E. M. (2020). DNA double-strand breaks induce H2Ax phosphorylation domains in a contact-dependent manner. *Nature Communications*, *11*, 3158.
102. de Luca, K. L., Rullens, P. M. J., Karpinska, M. A., de Vries, S. S., Gacek-Matthews, A., Pongor, L. S., Legube, G., Jachowicz, J. W., Oudelaar, M. A., & Kind, J. (2023). Genome-wide profiling of DNA repair proteins identifies higher-order coordination in single cells. BioRxiv, 2023.05.10.540169.
103. Wang, H., Maurano, M. T., Qu, H., Varley, K. E., Gertz, J., Pauli, F., Lee, K., Canfield, T., Weaver, M., Sandstrom, R., Thurman, R. E., Kaul, R., Myers, R. M., & Stamatoyannopoulos, J. A. (2012). Widespread plasticity in CTCF occupancy linked to DNA methylation. *Genome Research*, *22*, 1680–1688.
104. Maurano, M. T., Wang, H., John, S., Shafer, A., Canfield, T., Lee, K., & Stamatoyannopoulos, J. A. (2015). Role of DNA methylation in modulating transcription factor occupancy. *Cell Reports*, *12*, 1184–1195.
105. Wiehle, L., Thorn, G. J., Raddatz, G., Clarkson, C. T., Rippe, K., Lyko, F., Breiling, A., & Teif, V. B. (2019). DNA (de)methylation in embryonic stem cells controls CTCF-dependent chromatin boundaries. *Genome Research*, *29*, 750–761.
106. Guo, Y., Monahan, K., Wu, H., Gertz, J., Varley, K. E., Li, W., Myers, R. M., Maniatis, T., & Wu, Q. (2012). CTCF/cohesin-mediated DNA looping is required for protocadherin alpha promoter choice. *PNAS*, *109*, 21081–21086.
107. Monteagudo-Sanchez, A., Richard Albert, J., Scarpa, M., Noordermeer, D., & Greenberg, M. V. C. (2023). The embryonic DNA methylation program modulates the cis-regulatory landscape via CTCF antagonism. BioRxiv, 2023.11.16.567349.
108. Schmidt, D., Schwalie, P. C., Wilson, M. D., Ballester, B., Gonçalves, Â., Kutter, C., Brown, G. D., Marshall, A., Flicek, P., & Odom, D. T. (2012). Waves of retrotransposon expansion remodel genome organization and CTCF binding in multiple mammalian lineages. *Cell*, *148*, 335–348.
109. Grubert, F., Zaugg, J. B., Kasowski, M., Ursu, O., Spacek, D. V., Martin, A. R., Greenside, P., Srivas, R., Phanstiel, D. H., Pekowska, A., Heidari, N., Euskirchen, G., Huber, W., Pritchard, J. K., Bustamante, C. D., Steinmetz, L. M., Kundaje, A., & Snyder, M. (2015). Genetic control of chromatin states in humans involves local and distal chromosomal interactions. *Cell*, *162*, 1051–1065.
110. Katainen, R., Dave, K., Pitkänen, E., Palin, K., Kivioja, T., Välimäki, N., Gylfe, A. E., Ristolainen, H., Hänninen, U. A., Cajuso, T., Kondelin, J., Tanskanen, T., Mecklin, J.-P., Järvinen, H., Renkonen-Sinisalo, L., Lepistö, A., Kaasinen, E., Kilpivaara, O., Tuupanen, S., … Aaltonen, L. A. (2015). CTCF/cohesin-binding sites are frequently mutated in cancer. *Nature Genetics*, *47*, 818–821.

111. Delaneau, O., Zazhytska, M., Borel, C., Giannuzzi, G., Rey, G., Howald, C., Kumar, S., Ongen, H., Popadin, K., Marbach, D., Ambrosini, G., Bielser, D., Hacker, D., Romano, L., Ribaux, P., Wiederkehr, M., Falconnet, E., Bucher, P., … Dermitzakis, E. T. (2019). Chromatin three-dimensional interactions mediate genetic effects on gene expression. *Science*, *364*, eaat8266.
112. Fang, C., Wang, Z., Han, C., Safgren, S. L., Helmin, K. A., Adelman, E. R., Serafin, V., Basso, G., Eagen, K. P., Gaspar-Maia, A., Figueroa, M. E., Singer, B. D., Ratan, A., Ntziachristos, P., & Zang, C. (2020). Cancer-specific CTCF binding facilitates oncogenic transcriptional dysregulation. *Genome biology*, *21*, 247.

**How to cite this article:** Chang, L.-H., & Noordermeer, D. (2024). Permeable TAD boundaries and their impact on genome-associated functions. *BioEssays*, e2400137. https://doi.org/10.1002/bies.202400137